Since January 2020 Elsevier has created a COVID-19 resource centre with free information in English and Mandarin on the novel coronavirus COVID-19. The COVID-19 resource centre is hosted on Elsevier Connect, the company's public news and information website.

Immunity
Article

Promyelocytic Leukemia Zinc Finger Protein Regulates Interferon-Mediated Innate Immunity

Dakang Xu,[1,6] Michelle Holko,[2,6,7] Anthony J. Sadler,[1] Bernadette Scott,[1] Shigeki Higashiyama,[3] Windy Berkofsky-Fessler,[4,8] Melanie J. McConnell,[4,9] Pier Paolo Pandolfi,[5] Jonathan D. Licht,[4] and Bryan R.G. Williams[1,*]
[1]Monash Institute of Medical Research, Monash University, Melbourne, Australia
[2]Department of Preventive Medicine, Northwestern University, Chicago, IL 60611, USA
[3]Department of Biochemistry and Molecular Genetics, Ehime University Graduate School of Medicine, Shitsukawa, To-on, Ehime 791-0295, Japan
[4]Division of Hematology/Oncology, Department of Medicine, Northwestern University Feinberg School of Medicine, 303 E. Superior Street, Lurie 5-123, Chicago, IL 60611, USA
[5]Cancer Genetics Program, Beth Israel Deaconess Cancer Center and Department of Medicine and Pathology, Beth Israel Deaconess Medical Center, Harvard Medical School, Boston, MA 02215, USA
[6]These authors contributed equally to this work
[7]Present address: Gene Expression Omnibus, National Center for Biotechnology Information, National Institutes of Health, Bethesda, MD 20892, USA
[8]Present address: RNA Therapeutics Department, Hoffmann-La Roche Inc., Nutley, NJ 07110, USA
[9]Present address: Malaghan Institute of Medical Research, Wellington, New Zealand
*Correspondence: bryan.williams@med.monash.edu.au
DOI 10.1016/j.immuni.2009.04.013

SUMMARY

Interferons (IFNs) direct innate and acquired immune responses and, accordingly, are used therapeutically to treat a number of diseases, yet the diverse effects they elicit are not fully understood. Here, we identified the promyelocytic leukemia zinc finger (PLZF) protein as a previously unrecognized component of the IFN response. IFN stimulated an association of PLZF with promyelocytic leukemia protein (PML) and histone deacetylase 1 (HDAC1) to induce a decisive subset of IFN-stimulated genes (ISGs). Consequently, PLZF-deficient mice had a specific ISG expression defect and as a result were more susceptible to viral infection. This susceptibility correlated with a marked decrease in the expression of the key antiviral mediators and an impaired IFN-mediated induction of natural killer cell function. These results provide new insights into the regulatory mechanisms of IFN signaling and the induction of innate antiviral immunity.

INTRODUCTION

Type I interferons (IFNs) regulate diverse cellular functions by modulating the expression of a large family of IFN-stimulated genes (ISGs) through the activation of the Janus kinase (JAK) and signal transducers and activators of transcription (STAT) proteins (Haque and Williams, 1998; Stark et al., 1998). ISGs subsequently influence multiple pathways involved in cell stress responses, apoptosis, and proliferation and mediate diverse immune effects (Goh et al., 1999; Goodbourn et al., 2000). The potent immune response elicited by IFNs is exemplified by the establishment of an antiviral state that enabled their original discovery (Isaacs et al., 1957). This state relies on the induction and activation of numerous intrinsic antiviral factors, most notably the Mx GTPases, the 2′-5′-oligoadenylate-synthetase (OAS) system, ISG15, and protein kinase R (PKR) (Sadler and Williams, 2008). In addition, IFNs modulate distinct aspects of both innate and adaptive immunity, affecting the activities of macrophages, natural killer (NK) cells, dendritic cells, and T cells by enhancing ISG expression profiles, cell differentiation, cell trafficking, and antigen presentation. Because of the numerous effects of IFNs, they have been used therapeutically against a variety of diseases, including viral infections, immunomodulatory disorders, and hematological and solid tumors (Borden et al., 2007). The factors determining the outcome of IFN treatment, however, are not understood, and IFN therapy has had variable success. Although the essential JAK-STAT signal transduction pathway is well characterized, recent studies have revealed greater complexity in patterns of gene induction than initially envisaged (Chang et al., 2004; Tenoever et al., 2007; van Boxel-Dezaire et al., 2006). Here, we identified an IFN-mediated signal that leads to activation of the promyelocytic leukemia zinc finger protein (PLZF, encoded by *Zbtb16*) transcription factor that has fundamental consequences for the immune response.

PLZF is a member of the "BTB-POZ" (bric á brac, tramtrack, broad complex-poxvirus zinc finger) family of transcription factors and represses genes by recruiting several different corepressor complexes. Two recent reports describe a role for PLZF in the immune response as a transcription factor that is necessary for full function of natural killer T (NKT) cells (Kovalovsky et al., 2008; Savage et al., 2008), although the mechanisms were not investigated. Here, we present evidence that the role of PLZF in the immune response is broader than described in these reports. Contrary to the previous designation of PLZF as a repressor of transcription, we showed that PLZF was required for the induction of a subset of ISGs that are crucial in the ensuing immune response via the induction of the antiviral genes

and other ISG functions, including NK cell activity. These findings provide new insights into the regulation of IFN-mediated immunity.

RESULTS

PLZF Regulates Sensitivity to IFN

To determine the factors contributing to IFN sensitivity, we analyzed two renal cancer cell lines, differing markedly in their response to IFN (Holko and Williams, 2006), for their ISG profiles. Higher and more persistent expression of a subset of ISGs was noted in the IFN-sensitive RCC1 cells when compared with the relatively IFN-insensitive ACHN cells (Figure 1A). Correspondingly, RCC1 cells showed an increased IFN-mediated antiviral response (Figure S1 available online). No differences in established IFN-regulatory factors were apparent between the two cell lines (Holko and Williams, 2006). Therefore, to account for the differential regulation of this subset of ISGs, we analyzed the promoter proximal regions (1000 bp upstream of the ATG) for features that distinguished these genes from other ISGs that were synchronous between the two cell lines. It was found that genes differentially induced by IFNα treatment in the RCC1 cells exhibited an overrepresentation of DNA-binding motifs for the PLZF protein (Table S1). Cluster analysis showed the putative PLZF-binding sites were in proximity to sites occupied by essential STAT and IFN regulatory factors (IRFs), increasing the likelihood that these motifs were biologically relevant (Figure S2). To test this correlation between expression of ISGs with putative binding motifs and expression of the transcription factor, we assessed both cell lines for their expression of PLZF by immunoblot analysis. Consistent with a role for PLZF in the IFN response, the IFN-sensitive RCC1 cells expressed higher amounts of PLZF than the relatively IFN-insensitive ACHN cells (Figure 1B).

We further investigated this correlation between IFN sensitivity and expression of PLZF by using a monocytic U937 cell line stably transformed with a tetracycline-inducible PLZF-expressing construct (U937T:PLZF45) (McConnell et al., 2003). The ISG expression profiles of U937T:PLZF45 cells with and without tetracycline and IFNα were examined. PLZF expression alone resulted in the induction of a subset of ISGs and this was further enhanced by IFNα (Figure 1C and Table S2). The expression of representative ISGs was validated with real time RT-PCR (Figure 1D). Interestingly, an analysis of gene categories regulated by PLZF identified overrepresentation of immune response genes, particularly ISGs (Tables S3–S5), suggesting a particular role for PLZF in mediating the immune response.

PLZF Is Required for the IFN-Mediated Antiviral Response

To evaluate the contribution of PLZF to immune function, the IFN-mediated antiviral response was measured in embryonic fibroblasts (MEFs) derived from PLZF-deficient (*Zbtb16*$^{-/-}$) mice. Wild-type MEFs showed 100-fold greater IFN-mediated protection to infection with Semliki Forest Virus (SFV) than *Zbtb16*$^{-/-}$ MEFs (Figure 2A and Figure S3). The role of PLZF in the in vivo IFN-mediated antiviral response was assessed by infectious challenge of *Zbtb16*$^{-/-}$ and wild-type neonatal mice. Mice were infected with SFV at ten times the half-maximal tissue culture infectious dose ($TCID_{50}$), and resistance to the virus was measured as survival after infection. The survival curve of infected *Zbtb16*$^{-/-}$ mice closely parallels the wild-type, with all mice of both genotypes dead by 3.5 days after infection (Figure 2B) ($p > 0.05$). Appropriately, IFN pretreatment of mice for 6 hr before exposure to SFV afforded significant protection to wild-type mice, with 60% of infected neonates (18 of 30) surviving past 22 days. In contrast, IFN pretreatment did not protect the *Zbtb16*$^{-/-}$ mice from SFV infection, with no survival beyond 6 days after infection (Figure 2B). Viral loads in the organs from *Zbtb16*$^{-/-}$ and wild-type neonatal mice were measured 48 hr after infection with SFV. Consistent with the survival results, viral titers in the organs of *Zbtb16*$^{-/-}$ mice, including the lung, thymus, spleen, heart and liver, were up to 1,000-fold greater than their wild-type littermates (Figure 2C).

The observed immune impairment in *Zbtb16*$^{-/-}$ mice was not restricted to an increased susceptibility to infection by SFV. Wild-type and *Zbtb16*$^{-/-}$ mice had dramatically different susceptibility to infection with the encephalomyocarditis virus (EMCV). Intraperitoneal injection, with 500 plaque-forming units of EMCV, of 8- to 10-week-old mice showed that wild-type mice had significantly better survival over their *Zbtb16*$^{-/-}$ littermates (Figure 2D). These results show that PLZF is a key component of the innate immune response and is essential for resistance to virus infection in vivo.

PLZF Regulates Antiviral Effectors

In order to characterize the mechanism by which PLZF elicits an antiviral state, we analyzed IFN production and ISG expression in wild-type and *Zbtb16*$^{-/-}$ mice. Notably, the serum IFN concentrations were not obviously deficient in infected *Zbtb16*$^{-/-}$ mice (Figure 3A). This indicated that the observed virus susceptibility is independent of IFN production. The expression profile of a number of PLZF-dependent ISGs, identified in array experiments (Figures 1A and 1C and Table S2), was investigated ex vivo and in vivo. Importantly, the induction of the antiviral gene *Oas1g* by IFN was impaired in primary *Zbtb16*$^{-/-}$ bone-marrow-derived macrophages (BMMs) (Figure 3B). Given that OAS1 is an established effector for the antiviral action of IFN, specifically against SFV (Borden et al., 2007; Pestka et al., 1987), we measured its expression in different organs after IFN treatment and SFV infection. The induction of *Oas1g* was markedly impaired in splenocytes isolated from the *Zbtb16*$^{-/-}$ mice (Figures 3C–3E). Similarly, the antiviral ISGs *Rsad2* (also termed *Cig5* or *Viperin*) and *Ifit2* (or *Ifi54*) were impaired in *Zbtb16*$^{-/-}$ BMMs (Figure 3B) and splenocytes (data not shown), or SFV-infected organs from *Zbtb16*$^{-/-}$ mice (Figures 3C–3E). In keeping with the specificity of the PLZF response, expression of the PLZF-independent but IFN-regulated CCL5 (RANTES) transcript was not affected (Figure 3B). These data suggest that the increased susceptibility of *Zbtb16*$^{-/-}$ mice is due to a specific defect in the induction of antiviral genes.

A direct comparison of PLZF-independent and -dependent genes was made by comparison of the closely related *Ifit1* and *Ifit2* genes. Both IFIT1 and IFIT2 are strongly induced by IFN or viral infecton and are impaired in STAT1-deficient mice. These two genes are reported to have contrasting expression patterns in different tissues (Terenzi et al., 2007). Both genes contain ISRE binding sites in their promoter, but there is no PLZF-binding motif in the *Ifit1* promoter. Accordingly, *Ifit2* induction was lost in the

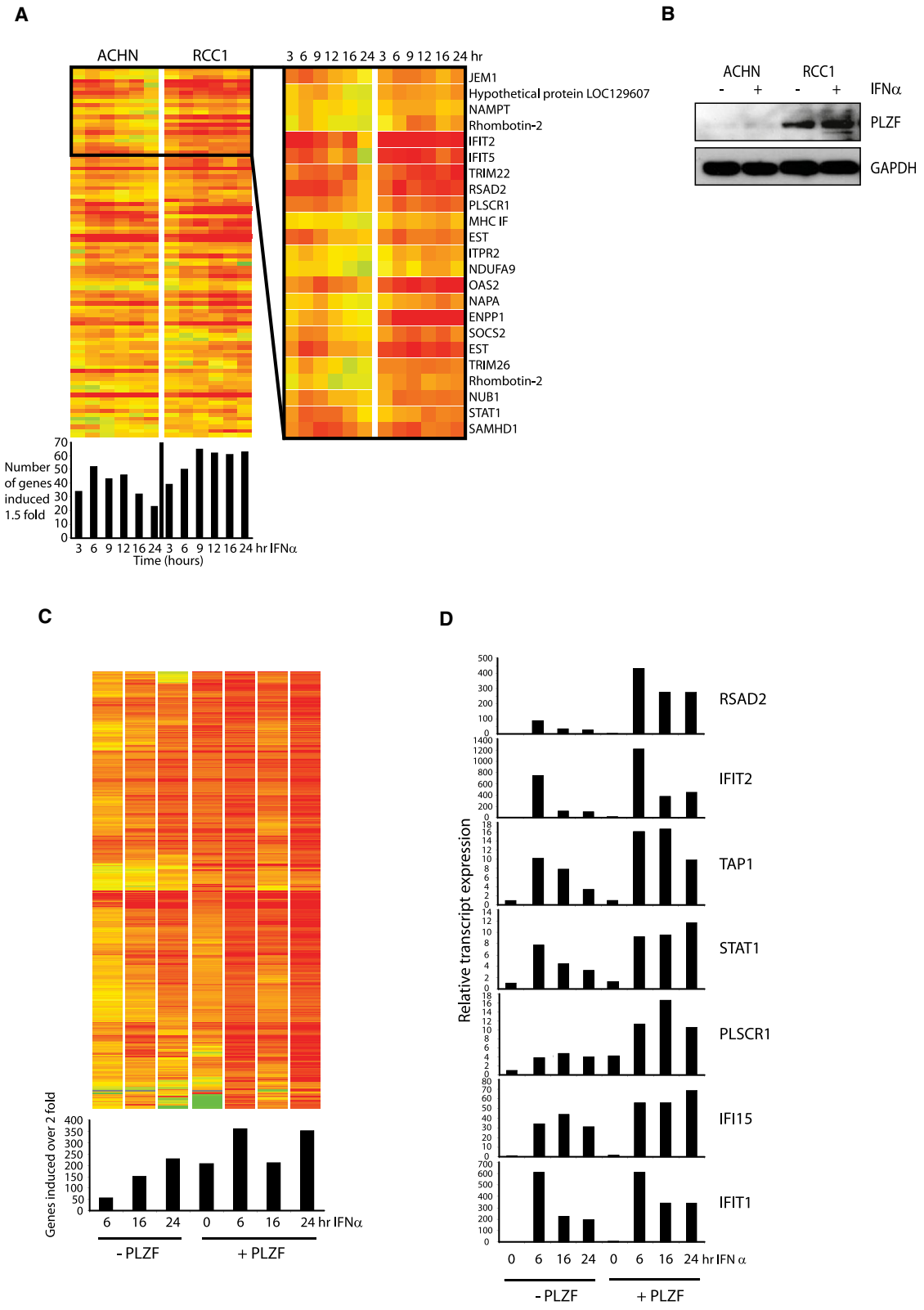
A
ACHN
RCC1
3 6 9 12 16 24 3 6 9 12 16 24 hr
JEM1
Hypothetical protein LOC129607
NAMPT
Rhombotin-2
IFIT2
IFIT5
TRIM22
RSAD2
PLSCR1
MHC IF
EST
ITPR2
NDUFA9
OAS2
NAPA
ENPP1
SOCS2
EST
TRIM26
Rhombotin-2
NUB1
STAT1
SAMHD1
Number of genes induced 1.5 fold
Time (hours)
IFNα
B
ACHN
RCC1
- + - +
IFNα
PLZF
GAPDH
C
Genes induced over 2 fold
6 16 24 0 6 16 24 hr IFNα
- PLZF
+ PLZF
D
Relative transcript expression
RSAD2
IFIT2
TAP1
STAT1
PLSCR1
IFI15
IFIT1
0 6 16 24 0 6 16 24 hr IFN α
- PLZF
+ PLZF

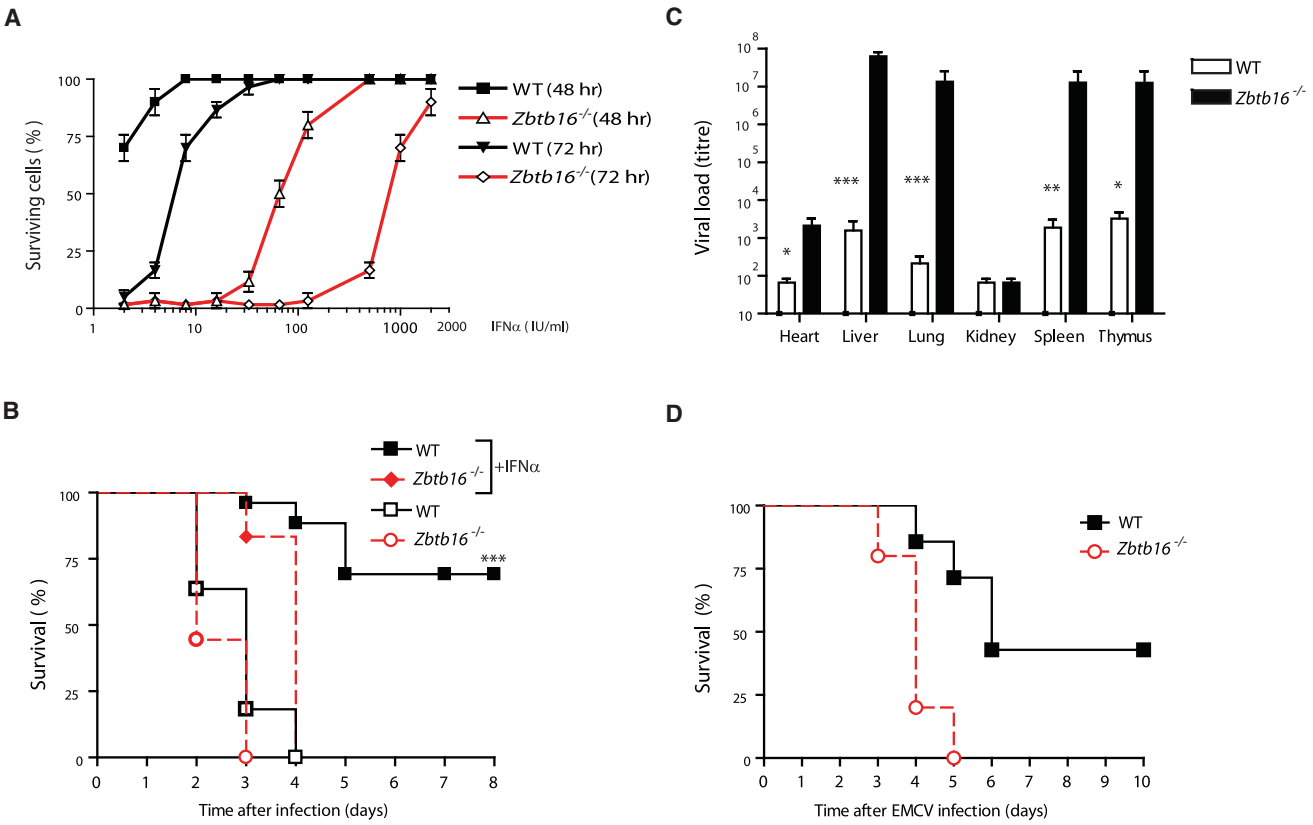

Figure 2. PLZF Is Required for the IFN-Mediated Antiviral Response

(A) Antiviral assay on wild-type (WT) and PLZF-deficient (*Zbtb16*$^{-/-}$) MEFs infected with SFV for 48 and 72 hr. IFNα1 was added to cells at the indicated concentrations 16 hr prior to infection. The titers of IFNα required to protect cells from the cytopathic effects of SFV infection are expressed as percentage survival. Error bars represent 1 standard deviation (SD).

(B) Survival after SFV infection of neonatal mice. WT or *Zbtb16*$^{-/-}$ neonatal mice between 5 and 6 days of age were divided into two groups: either a control group for each genotype (without IFN pretreatment: WT, n = 11; *Zbtb16*$^{-/-}$, n = 8) or an IFN pretreatment group (WT, n = 30; *Zbtb16*$^{-/-}$, n = 12). The IFN pretreatment group was given 5000 IU IFNα; the control group was injected with PBS. After 6 hr, all mice were infected with SFV at 30× $TCID_{50}$ and were monitored. Without IFN treatment, there was no significant difference in resistance to infection with SFV at 30× $TCID_{50}$ in WT and *Zbtb16*$^{-/-}$ neonatal mice ($p > 0.05$, log-rank test). With IFN pretreatment, wild-type mice showed more resistance in response to SFV than *Zbtb16*$^{-/-}$ mice (***$p < 0.001$, log-rank test).

(C) Increased virus replication in *Zbtb16*$^{-/-}$ mice. Neonatal mice from *Zbtb16*$^{+/-}$ matings were injected with IFNα1 and SFV between 5 and 6 days of age. Neonates were monitored for 72 hr, at which time they were killed and organs were collected. Viral titers were measured by CPE assay and expressed as mean log titer ± SEM. *$p < 0.05$; **$p < 0.01$; and ***$p < 0.001$; *Zbtb16*$^{-/-}$ neonatal mice (n = 7) versus their wild-type littermates (n = 8; Mann-Whitney rank sum tests).

(D) *Zbtb16*$^{-/-}$ mice also show increased susceptibility to lethal infections with EMCV. *Zbtb16*$^{-/-}$ mice (n = 5) and WT littermate controls (n = 7) were injected i.p. with 500 pfu of EMCV and monitored for survival. *Zbtb16*$^{-/-}$ mice died after a mean survival time of 4 days, whereas WT mice survived for a mean of 7 days ($p = 0.009$).

absence of PLZF, whereas *Ifit1* was still induced by IFNα in *Zbtb16*$^{-/-}$ mice (Figure 3F). Furthermore, analysis of the expression of PLZF in different tissues showed a strong correlation between PLZF expression and *Ifit2* induction in response to IFNα (Figure 3F). Hence, the different expression patterns of these two related ISGs probably depend upon their separate regulation by PLZF. Although expression of IFIT1 is largely independent of PLZF, a degree of PLZF dependence is noted in the lung of mice, suggesting that PLZF might still contribute indirectly to inducer-specific ISG regulation.

Figure 1. PLZF Regulates Sensitivity to IFN

To determine factors contributing to IFN sensitivity, two RCC cell lines, ACHN and RCC1, were analyzed for ISG expression and response to IFN treatment.

(A) ISGs induced by 1000 IU/ml IFNα-2b at any one time point in either ACHN or RCC1 cells. Red indicates induced genes, yellow indicates no change, and green indicates repressed genes (top-left panel). The bar graph below shows the number of genes induced at least 1.5-fold for each sample. A total of 22 ISGs with higher and more persistent expression in the IFN-sensitive RCC1 cells is shown (top-right panel).

(B) Immunoblot analysis of PLZF expression in ACHN and RCC1 cells in the presence or absence of IFNα. Data are representative of three independent experiments.

(C) ISGs expressed in PLZF-inducible U937T cells, treated with IFNα for 6, 16, and 24 hr in the presence and absence of PLZF expression (24 hr after tetracycline withdrawal). The bar graph below shows the number of genes induced at least 2-fold for each sample.

(D) Expression of select genes (Table S4) was verified with SYBR Green real-time RT-PCR. Data are shown as mRNA expression normalized to the GAPDH RNA. Data were confirmed in three independent experiments.

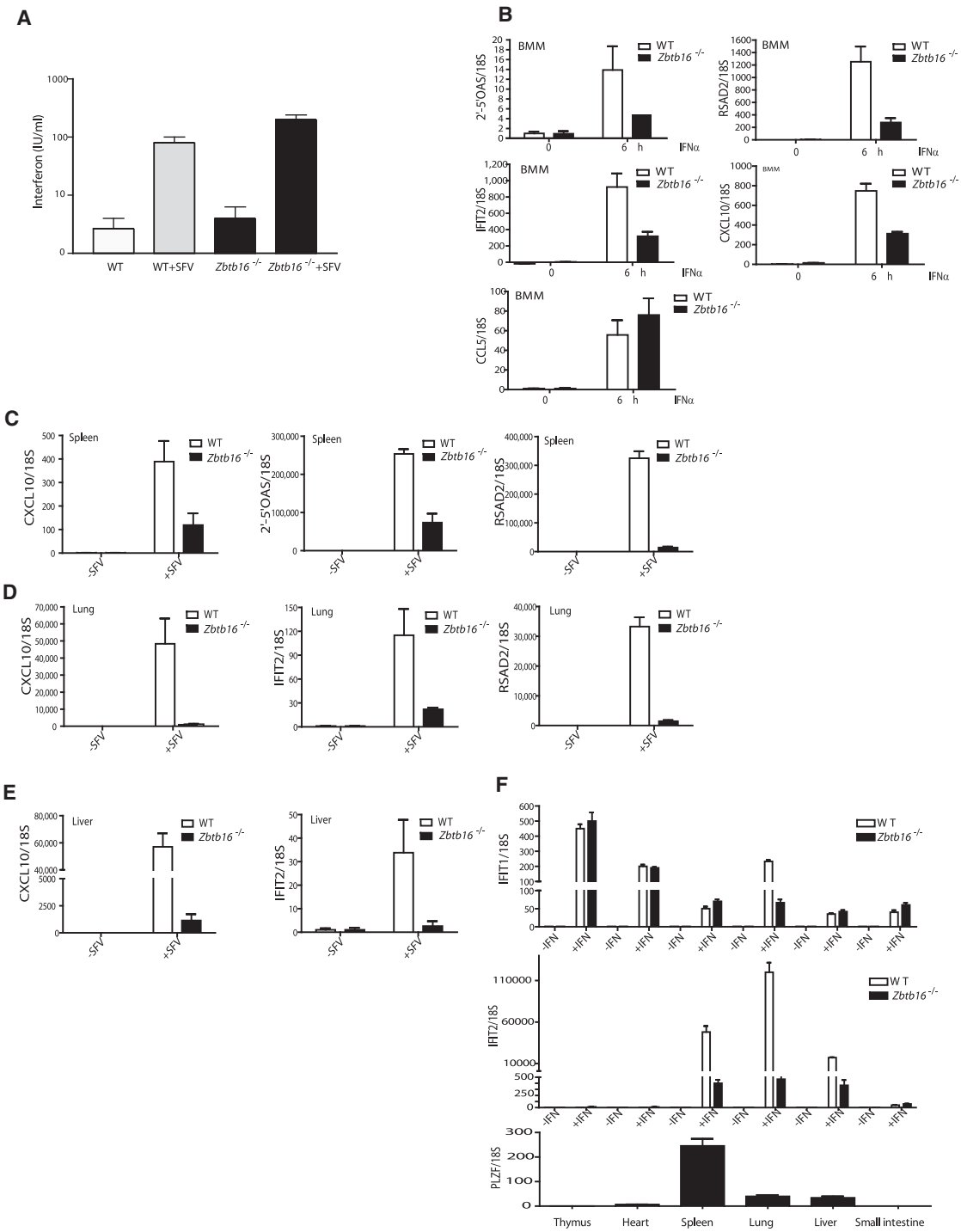

Figure 3. PLZF Regulates Antiviral Effectors

(A) Serum IFN concentrations from neonatal wild-type (WT) and *Zbtb16*$^{-/-}$ mice injected with IFNα, with and without SFV injection. IFN was measured after 48 hr by CPE reduction assay. Bar graphs show mean ± SD of five mice for each group.

(B) IFN-induced ISG expression of the antiviral IFN effectors OAS1, RSAD2, and IFIT2, and the chemokines CXCL10 (IP-10) and CCL5 (RANTES) were measured in WT or *Zbtb16*$^{-/-}$ BMMs after IFNα treatment for 6 hr. Data are shown as mRNA expression normalized to the 18S RNA. Bar graphs show mean ± SD of three independent experiments.

(C–E) The mRNA expression of the chemokine CXCL10 (IP-10) and the antiviral ISGs OAS1, RSAD2, and IFIT2 was measured in predominantly NK cell-rich organs (spleen, liver, and lung) from WT and *Zbtb16*$^{-/-}$ neonatal mice after IFNα treatment and SFV infection. RNA samples were analyzed for ISG expression with a custom ISG probe.

Data are representative of three independent experiments (mean ± SEM; A–E).

Interestingly, measurement of CXCL10 expression in the organs after IFN treatment only, or IFN treatment and SFV infection, revealed that the induction of CXCL10 by IFNα was impaired in primary *Zbtb16*$^{-/-}$ BMMs (Figure 3B). CXCL10 was also markedly impaired in splenocytes, liver, and lung isolated from the SFV-infected *Zbtb16*$^{-/-}$ mice (Figures 3C–3E). CXCL10 (or IP-10) has been associated with NK cell activity and the resulting protection from virus infection (Biron et al., 1999; Thapa et al., 2008). Therefore, an additional means by which PLZF might regulate sensitivity to virus, besides inducing direct antiviral effectors, could be a result of IFN-mediated activation of NK cells via ISGs such as CXCL10. This possibility was investigated.

NK Cell Activation Is Impaired in *Zbtb16*$^{-/-}$ Mice

Two recent reports have shown that PLZF affects NKT cell activity (Kovalovsky et al., 2008; Savage et al., 2008). However, analysis of PLZF expression in immune cells with the human and mouse microarray database (Gene Expression Omnibus [GEO] accession number GSE 6887) revealed that PLZF was also expressed in human NK cells (Figure S4). Furthermore, we demonstrated that PLZF was expressed in mouse NK cells by sorting different spleen lymphocyte populations with FACS (NK1.1^{+}CD3^{-}) and then analyzing their gene expression (Figure 4A). This analysis shows comparatively little expression in CD3^{+}NK1.1^{-} T cells and no detectable transcript in B cells. Consequently, we investigated the effect of the loss of PLZF on NK cell function. FACS analysis of splenocytes showed there were equivalent numbers of NK cells in wild-type and *Zbtb16*$^{-/-}$ mice, with NK cells constituting 2%–3% of total splenocytes (Figure 4B). We investigated the effector function of NK cells from wild-type and *Zbtb16*$^{-/-}$ mice by testing their cytolytic activity against the NK-sensitive target cell line YAC-1 (Fehniger et al., 2007; Shey and Ballas, 2008). After treatment with poly(I:C), which activates NK cells through the IFNα signaling pathway, *Zbtb16*$^{-/-}$ NK cells were impaired in their ability to spontaneously lyse YAC-1 cells (Figure 4C, top panel). Moreover, when activated in vivo with IFNα, the ability of *Zbtb16*$^{-/-}$ NK cells to subsequently lyse YAC-1 target cells was also markedly impaired (Figure 4C, bottom panel). These results demonstrate that PLZF is required for NK cell effector function and also suggest that PLZF may regulate the expression of target genes involved in NK cytolytic activity. Given that cytokine-induced activation of NK cells results in a dramatic increase in the expression of Granzyme B (GzmB), we examined the ability of poly(I:C) and IL-2 to induce GzmB protein expression in murine splenic NK cells. Mice were injected intraperitoneally with poly(I:C) or PBS, and splenic NK cells were analyzed after 24 hr for GzmB expression by flow cytometry. Wild-type spleens of poly(I:C)-injected mice had a markedly higher percentage of NK cells positive for GzmB than spleens of *Zbtb16*$^{-/-}$ mice (Figure 4D). The reduced amount of GzmB is consistent with a reduced ability to lyse target cells. Activation of NK cells in vitro with IL-2 induced equivalent amounts of GzmB in either genotype (data not shown). Therefore, the role of PLZF in the induction of GzmB is through IFNα, rather than other cytokines.

PLZF Directly Regulates the Promoters of a Subset of ISGs

Next we sought to define the mechanism by which PLZF enhanced the expression of a specific subset of ISGs. Treatment of U937T:PLZF45 cells with the transcriptional inhibitor actinomycin D suggested that the induction of selected ISGs by PLZF is a primary transcriptional event (Figure S5). Promoter regions from the PLZF-regulated transcripts *Rsad2* and *Ifit2* were fused to luciferase and activity was measured after IFN treatment. Overexpression of PLZF in RCC1 or ACHN cells produced a dose-dependent induction of the reporter promoters. This effect was further enhanced by IFNα treatment (Figures 5A–5C). Correspondingly, induction of the *Rsad2* promoter was impaired in cells with PLZF expression reduced by RNA interference (Figure 5D). Reporter constructs confirm the requirement to colocate ISRE and PLZF-binding sites in the promoters of PLZF-regulated ISGs (Figure S6). A direct association of PLZF with the promoters of *Rsad2* and *Ifit2* was demonstrated by chromatin immunoprecipitation assays in the RCC1 and U937T:PLZF45 cell lines. Moreover, the association of PLZF to the *Rsad2* and *Ifit2* promoters was dramatically enhanced by IFN treatment (Figure 5E and Figure S7).

IFN Activates PLZF

The observed IFN-enhanced association of PLZF with select ISG promoters could occur through direct posttranslational modification of PLZF and/or modification of transcriptional cofactors. To investigate the former possibility, we immunoprecipitated PLZF from control and IFNα-treated U937T:PLZF45 cells and probed the acetylation or phosphorylation state of the protein by immunoblotting. Although acetylation has been reported to be important for DNA binding of PLZF (Guidez et al., 2005), no change in the acetylation state was detected (data not shown). However, PLZF was found to be phosphorylated at serine and tyrosine residues, with tyrosine phosphorylation correlating with temporal treatment with IFNα (Figure 6A). PLZF encodes two types of conserved domain, a BTB domain at the N terminus and nine repeated zinc finger domains at the C terminus. Because BTB domains have been shown to be crucial for homodimerization and protein-protein interaction (Dong et al., 1996), we chose to focus on residues within this domain. Through alignment of the amino acid sequence of PLZF with BTB domains from various other proteins and by analysis with prediction programs (NetPhos 2.0, Department of Systems Biology, Technical University of Denmark), several putative phosphorylated residues within the BTB domain of PLZF were identified along with residues previously shown to be crucial for PLZF to function as a transcriptional repressor (Figures S8–S10). We mutated residues in PLZF to test their significance in the IFNα-mediated induction of the *Rsad2* promoter. This approach identified the tyrosine at position 88 and a serine residue at amino acid 76 to

(F) PLZF expression correlates with IFIT2 induction in response to IFNα in WT and *Zbtb16*$^{-/-}$ mice. PLZF expression was determined in multiple organs including thymus. Mice were then injected with PBS or IFNα (1 × 10^{5} IU), and after 8 hr, multiple organs were removed and RNA was extracted. IFIT1 and IFIT2 mRNA expression was analyzed by real-time RT-PCR, with a custom ISG probe (top panels). Data are representative of three independent experiments (mean ± SEM).

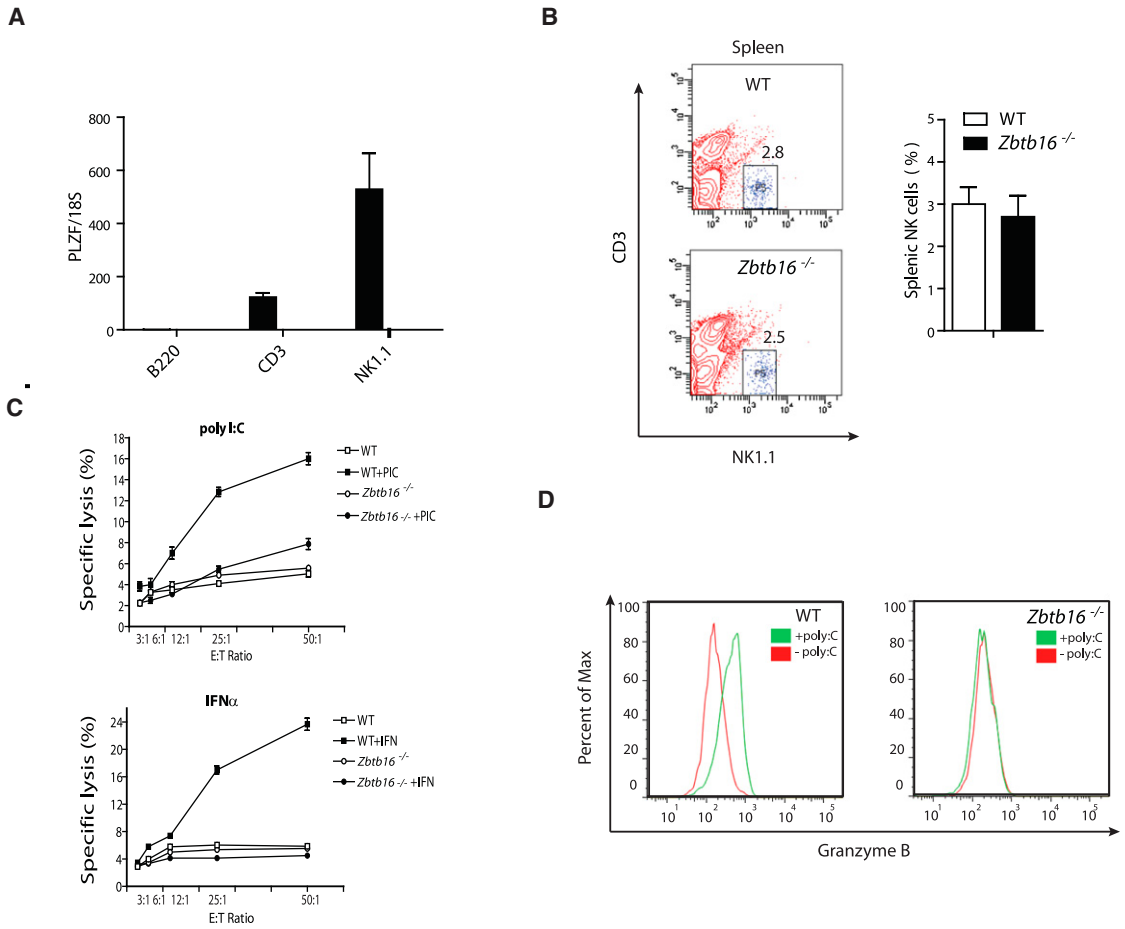

Figure 4. NK Cell Activation Is Impaired in *Zbtb16*$^{-/-}$ Mice

(A) Expression of the gene encoding PLZF in mouse spleen lymphocytes. Quantitative RT-PCR analysis of PLZF transcripts, relative to the expression of 18S mRNA, in various sorted lymphocyte populations. Results are the means of three independent experiments (mean ± SD).

(B) NK cell numbers in the spleens of *Zbtb16*$^{-/-}$ and wild-type (WT) mice. NK cell populations (NK1.1^{+}CD49b^{+}) were assessed by flow cytometry. Data (mean ± SD) are representative of three experiments.

(C) Diminished NK cell activity in *Zbtb16*$^{-/-}$ mice. Splenocytes labeled with carboxy-fluorescein diacetate succinimidyl ester (CFSE) were incubated for 4 hr with NK-sensitive YAC-target cells at the indicated effector-to-target (E:T) ratios. Lysed cells were detected by 7-amino-actinomycin D (7-AAD) incorporation. Mice were injected intraperitoneally with 10 μg of poly(I:C) 24 h (top panel), or IFNα1 2 days (bottom panel) before splenocyte isolation. Data are representative of four independent experiments (mean ± SD).

(D) WT and *Zbtb16*$^{-/-}$ mice were injected i.p. with 50 μg poly(I:C) or PBS (control), and after 24 hr, splenic NK1.1^{+} CD3^{-} NK cell expression of intracellular Gzmb was analyzed by flow cytometry. Flow cytometry data representative of at least five independent experiments are shown in the WT, with a significant increase in the percentage of NK cells positive (mean ± SD) for Gzmb after poly(I:C) injection.

be important for induction of *Rsad2* (Figure 6C). Consistent with these promoter reporter assays, phosphorylation analysis of the full-length mutant protein (S76A) indicated that the residue at position 76 was the sole phosphoserine residue of importance in IFN-mediated activation (Figure 6B). Two additional mutations, R49D and L103E, which had previously been demonstrated to constitute important structural components on either surface of the BTB domain, had opposing effects upon ISG induction. As anticipated, the L103E mutation impaired activation of *Rsad2*. Surprisingly, mutation of R49 induced the *Rsad2* reporter. Although the structure of the charged pocket that surrounds the R49 residue had been demonstrated to be critical for PLZF to function as a transcriptional repressor, these results suggest that other residues of the BTB domain on the lateral surface, where L103 lies, may be more pertinent to the role of PLZF as a transcription inducer.

To identify the kinase that phosphorylates PLZF, we conducted reporter assays (using *Rsad2*-luciferase) in cells treated with kinase inhibitors or cell lines defective in components of the IFN signaling pathway. Predictably, mutations in the JAK-STAT pathway led to the impairment of all IFN signaling for PLZF-regulated ISGs (Figure S11). Treatment of HeLa cells with pharmacological inhibitors of ERK (PD98059), JNK (SP600125), p38 (SB203580), Src (AZD0530), PI3K (AS-252424), or JAK2 (JAK2 inhibitor II), followed by stimulation with IFN, points to JNK as a possible PLZF kinase (Figures 6D and 6E), or at least a critical kinase in the pathway, and supports the importance of serine phosphorylation of the protein (Figure 6B).

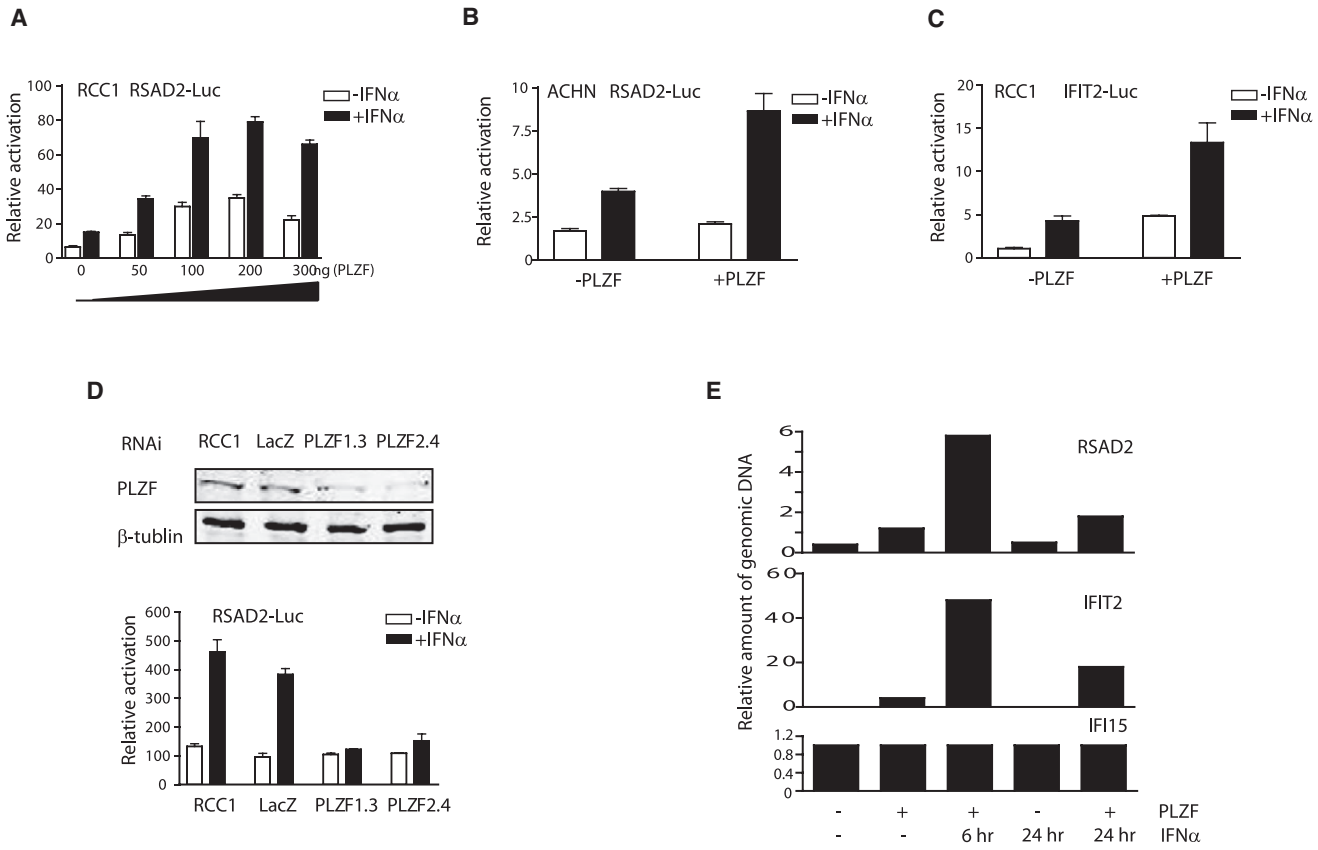

Figure 5. PLZF Directly Regulates the Promoters of a Subset of ISGs

(A–C) Overexpression of PLZF in RCC1 and ACHN cells induces RSAD2 and IFIT2 promoter activity. RCC1 or ACHN cells were cotransfected with a PLZF expression plasmid and RSAD2-Luc or IFIT2-Luc promoter reporter constructs, then treated with IFNα1 (500 IU/ml of IFNα1). The luciferase values were obtained in at least three independent experiments.

(D) Immunoblot analysis of PLZF in RCC1 cells expressing targeted or control miRNA (top panel). Luciferase assay for RSAD2 promoter induction in RCC1 cells expressing miRNAs targeting PLZF (PLZF1.3 and PLZF2.4) or the control miRNA targeting LacZ (LacZ) then stimulated with IFNα (bottom panel) is shown. Data are representative of three independent experiments (mean ± SD; A–D).

(E) Chromatin from PLZF-inducible (FLAG-tagged) U937T cells grown in the presence or absence of tetracycline (24 hr) and IFNα (1,000 U/ml for 6 or 24 hr) was immunoprecipitated with a FLAG antibody. Promoters of PLZF-dependent RSAD2, IFIT2, and PLZF-independent IFI15 were amplified from the immunoprecipitated PLZF-FLAG chromatin with SYBR Green quantitative RT-PCR. Data represent the relative amount of genomic DNA from each promoter normalized to 10% input DNA at each point.

PLZF Regulates ISGs through Interaction with HDAC1 and PML

IFN-enhanced association of PLZF with select ISG promoters could also occur through regulation of transcriptional cofactors. Accordingly, we sought to measure IFN-induced changes in known PLZF cofactors. Transcriptional repression by PLZF is sensitive to inhibitors of deacetylation, and PLZF physically interacts with both class I and II histone deacetylases (HDACs) via the BTB domain (Ahmad et al., 1998; Chauchereau et al., 2004; David et al., 1998). In accord with a requirement for HDAC activity for transcriptional activation of ISGs by PLZF, treatment of cells with the HDAC inhibitor trichostatin A (TSA) blocked induction of selected ISGs in the PLZF-inducible U937T:PLZF45 cells or BMMs (Figures 7A and 7B). An association between the class I histone deacetylase HDAC1 and PLZF was shown by coimmunoprecipitation of overexpressed FLAG-tagged PLZF in HEK293 cells. Notably, an association with the class II histone deacetylase HDAC4 was not detected under the same conditions (Figure 7C). This association between PLZF and HDAC1 was confirmed with endogenous protein under more physiologically relevant conditions in primary BMMs (Figure 7D). As an additional measure of co-operation between PLZF and HDAC1, the effect of coexpressing PLZF and HDAC1 upon the *Rsad2* reporter was measured in IFN-responsive RCC1 cells. Appropriately, coexpression of PLZF with HDAC1 enhanced the induction of the ISG promoter by IFNα to a greater degree than that observed with either protein expressed alone. Moreover, treatment with TSA blocked the additive effect of PLZF and HDAC1 (Figure 7E).

A second transcription factor reported to associate with PLZF is the promyelocytic leukemia protein (PML) (Koken et al., 1997; Regad and Chelbi-Alix, 2001). Of relevance to this study, PML mediates the formation of nuclear bodies that are crucial in the IFN response. More directly, it has been established that the antiviral response is reduced in PML-deficient MEFs (Day et al., 2004). To determine whether PML is a cofactor in PLZF-mediated

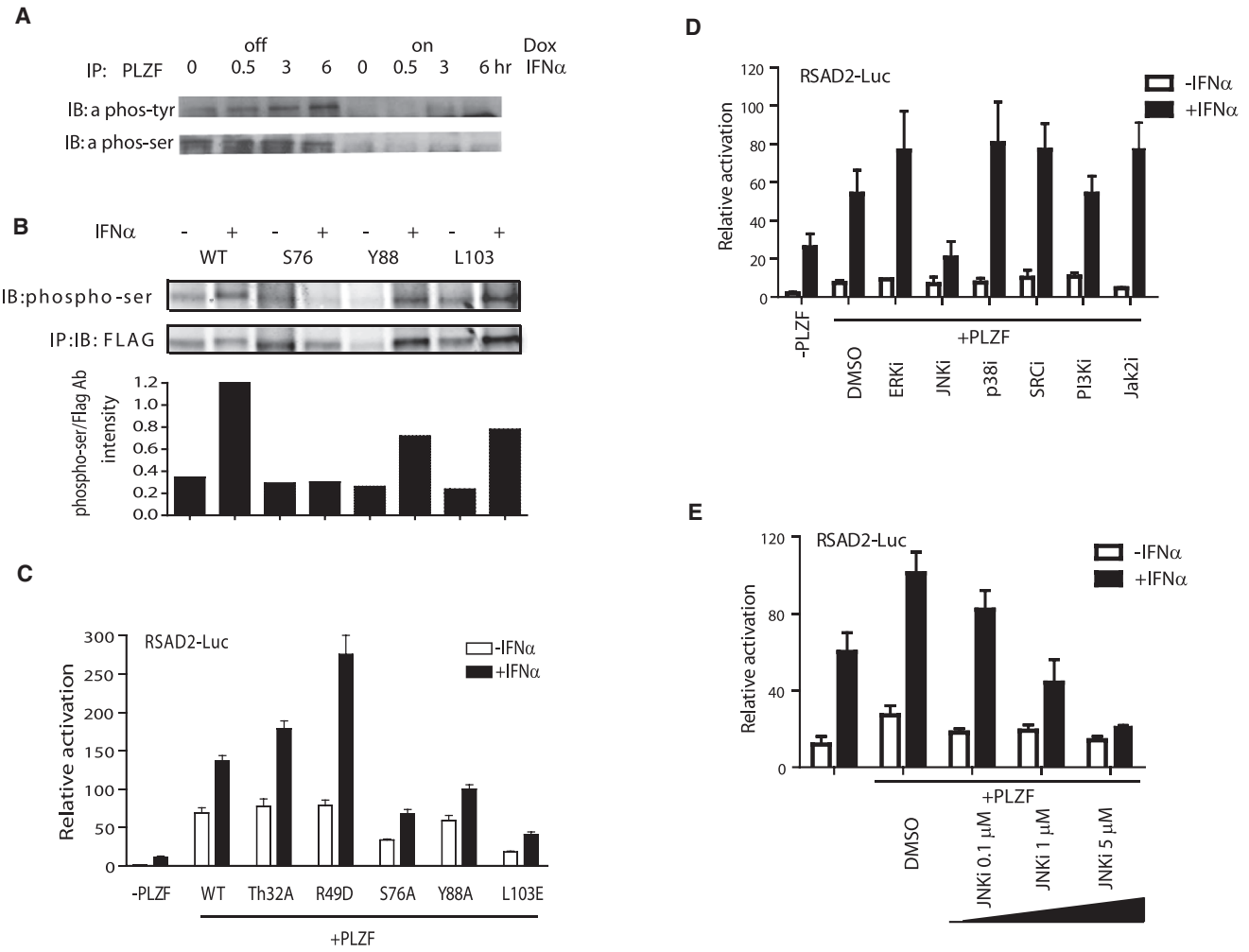

Figure 6. IFN Activates PLZF

(A) Phosphorylation of wild-type PLZF after IFNα stimulation. PLZF-inducible U937T cells grown in the presence or absence of tetracycline for 24 hr and IFN for the times indicated were immunoprecipitated (IP) with a PLZF antibody and immunoblotted (IB) with phospho-Tyr Ab (top panel) or phospho-Ser Ab (bottom panel).

(B) Serine76 is required for PLZF phosphorylation in response to IFNα. HeLa cells were transiently transfected with wild-type (WT) FLAG-PLZF or various mutant PLZF expression plasmids; this was followed by IFNα treatment, immunoprecipitation (IP) with the FLAG antibody, and immunoblotting (IB) with a phosphoserine or FLAG antibody, as indicated. The bar graph shows the proportion of phosphoserine residues on WT and mutant PLZF, treated with or without IFNα.

(C) Luciferase assay for RSAD2 promoter induction in lysates of RCC1 cells transfected with wild-type (WT) or indicated mutant PLZF expression plasmids, followed by stimulation with IFNα. The values obtained from at least three independent transfection experiments were normalized to TK Renilla.

(D) HeLa cells were transfected with PLZF expression and RSAD2 promoter reporter plasmids. The cells were then either left untreated or were treated with inhibitors of ERK (5 μM PD98059), JNK (1 μM SP600125), p38 (2.5 μM SB203580), Src (1 μM AZD0530), PI3K (1 μM AS-252424), or JAK2 (0.5 μM JAK2 inhibitor II); they subsequently underwent IFNα stimulation for 8 hr before RSAD2 promoter reporter activity in cell lysates was measured.

(E) Luciferase assay for RSAD2 promoter induction in lysates of HeLa cells overexpressing PLZF and pretreated with different concentrations of JNK inhibitor, followed by IFNα stimulation. Data are representative of three independent experiments (mean ± SD; C–E).

activation of ISGs, we performed coimmunoprecipitation assays on lysates from the IFN-responsive HeLa cells, overexpressing PLZF-tagged constructs, or on endogenous PLZF from primary BMMs. PLZF was found to interact with PML in both cell types after IFNα treatment (Figures 7F, 7G; Figures S12 and S13). Importantly, PML has been demonstrated to alter the cellular location of PLZF (Koken et al., 1997). To show whether the association between PLZF and PML, detected by immunoprecipitation, correlated with colocalization of the proteins within nuclear bodies, we performed confocal microscopy with fluorescently tagged proteins in RCC1 cells treated with or without IFNα. Indirect immunofluoresence confirmed that PLZF localized with PML after IFN stimulation (Figure 7H). The reported induction of PML by IFN does not account for the observed colocalization, given that the amounts of PML did not significantly increase over the duration of this experiment (Figure S14). Together, these data show that IFN treatment induces phosphorylation of PLZF, plausibly by JNK, and interaction with both HDAC1 and PML to mediate association of the complex with PLZF-binding sites in gene promoters to induce specific ISGs.

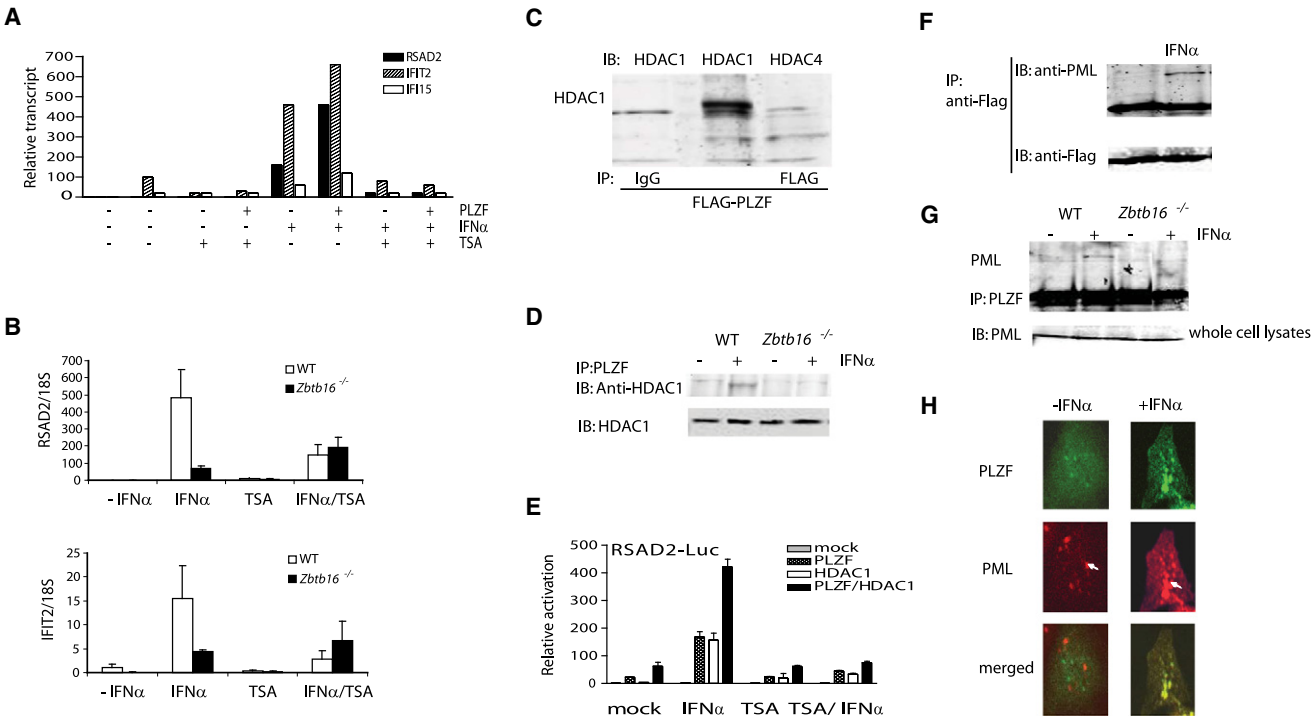

Figure 7. PLZF Regulates ISGs through Interaction with HDAC1 and PML

(A) Relative transcript levels of RSAD2, IFIT2, and IFI15, after tetracycline withdrawal for the PLZF-inducible U937T cells, treated with TSA prior to huIFN-α2b. RNA was extracted and ISG expression was measured by real time RT-PCR. Data are shown as RSAD2, IFIT2 and IFI15 RNA levels normalized to GAPDH RNA.

(B) Transcript levels of RSAD2 and IFIT2 measured by real-time RT-PCR in wild-type (WT) and *Zbtb16*$^{-/-}$ BMMs. Cells were treated with IFNα, TSA alone, or IFNα and TSA. Data are shown as RNA expression levels normalized to 18S RNA and are representative of three independent experiments (mean ± SEM; A and B).

(C) Cell lysates prepared from HEK293T cells transiently transfected with FLAG-PLZF, immunoprecipitated (IP) with the FLAG antibody, and immunoblotted (IB) with anti-HDAC1 or anti-HDAC4.

(D) WT and *Zbtb16*$^{-/-}$ BMMs were incubated in the absence or presence of IFNα. Cell lysates were immunoprecipitated with PLZF antibody and immunoblotted with HDAC1 antibody.

(E) RCC1 cells expressing PLZF and HDAC1 alone or in combination were stimulated with IFNα, TSA alone, or IFNα and TSA. Relative RSAD2 promoter activity was determined by activity of RSAD2 luciferase assay and normalization to TK Renilla. Data are representative of three independent experiments (mean ± SD).

(F) HeLa cells were transiently transfected with FLAG-PLZF; this was followed by IFNα treatment, immunoprecipitation with the FLAG antibody, and immunoblotting with a PML or PLZF antibody, as indicated.

(G) WT and *Zbtb16*$^{-/-}$ BMMs were incubated in the absence or presence of IFNα, immunoprecipitated with PLZF antibody, and immunoblotted with PML antibody.

(H) Confocal images of RCC1 cells transiently expressing PLZF-CFP with and without IFNα treatment. Arrows indicate the colocalization of PLZF with PML. Images are representative of four independent experiments.

DISCUSSION

Recent studies have shown that type I IFN signaling is more complex than initially recognized, activating different specific signals and patterns of gene expression (van Boxel-Dezaire et al., 2006). The response via the canonical JAK-STAT pathway alone is not sufficient to explain all the biological effects of type I IFN. Accordingly, other kinases, including PI3K and MAP kinase, lead to the activation of additional transcription factors such as NF-κB, AP-1, IRFs, and PU.1, which interact with STATs at interferon-stimulated response elements (ISREs) via ISGF3 or other IRFs to regulate ISGs. We showed that the transcription factor PLZF is a regulator of the IFN response. PLZF induced a specific subset of ISGs with PLZF-binding sites in proximity to ISRE. Gene array, chromatin immunoprecipitation (ChIP) assays, and promoter reporter experiments demonstrated that PLZF directly occupied these select promoter sequences and that this activity was IFN dependent. In this study, analysis of all genes induced by PLZF showed a predominance of ISGs, explicitly implicating PLZF in positively modulating the IFN pathway.

Although PLZF has been designated as a transcriptional repressor, our observation that PLZF promotes ISG transcription is not without precedence (Labbaye et al., 2002; Senbonmatsu et al., 2003). The mechanism for transcriptional repression by PLZF is thought to involve constraint of the accessibility of the gene to transcriptional machinery, via chromatin remodeling by acetylation involving the nuclear corepressor complex (NCoR) and HDACs, particularly HDACs 1 and 4 (Chauchereau et al., 2004; David et al., 1998; Guidez et al., 2005; Hong et al., 1997; McLoughlin et al., 2002). Although HDACs are generally considered as corepressors, HDAC1 could serve as a coactivator for the glucocorticoid receptor (Qiu et al., 2006). More relevant to our findings, we and others found that inhibition of HDAC1 perturbed IFN-induced transcription and antiviral responses.

Moreover, data generated from HDAC1-deficient cells show that this protein is required for the efficient activation of ISGs (Chang et al., 2004; Zupkovitz et al., 2006). Also, HDAC1 but not HDAC4 associated with STAT1 and STAT2 to positively activate expression of the ISG3-dependent transcriptional response. Correspondingly, we detect an association between PLZF and HDAC1, not HDAC4, upon stimulation with IFNα, leading us to propose that HDAC1 is key to PLZF's role as a transcriptional enhancer. Similarly to HDAC1, a second PLZF cofactor, PML, is indispensable for the IFN response (Handwerger and Gall, 2006). Appropriately, PML is induced by IFN through an ISRE and an IFN-γ activation site (GAS) motif in its promoter, and the number and intensity of nuclear bodies increase in response to IFN (Stadler et al., 1995). More directly, it has been established that the antiviral response is reduced in PML-deficient MEFs (Day et al., 2004). We demonstrate here that PLZF and PML associate and that this interaction is also modulated by IFN.

Although the precise mechanism modulating the association between PLZF and its cofactors has not been established, it is predicted to be mediated by the BTB domain of PLZF (Melnick et al., 2000b). This domain acts as a homodimerization motif that is essential for the repressor function of PLZF and its localization in nuclear bodies. (Melnick et al., 2000a) Our results suggest that this domain is also key for its transcriptional enhancer function. However, our observations indicated differences in how the BTB domain mediates repressor or enhancer activities of PLZF. Mutation of the residue at position 49 in the BTB domain of PLZF, shown to be essential for repressor activity, had the contradictory effect of further enhancing ISG expression. Mutation of another key structural residue, on the lateral face of the BTB domain at position 108, recapitulated the loss of function as a repressor. This implies that different regions of PLZF mediate repressor or enhancer functions. Because we found an interaction between PLZF, PML, and HDAC1 only after IFN stimulation, it seems likely that IFN signaling affects the state of one or all of these proteins. Informatively, the apparent paradoxical function of HDAC1 as a corepressor or coactivator appears to be regulated by acetylation of the protein itself (Melnick et al., 2000a). It is also reported that PLZF is both acetylated and phosphorylated (Ball et al., 1999; Guidez et al., 2005). In this study, PLZF was found to be phosphorylated at serine and tyrosine residues in response to IFN, and we identified a serine residue (Ser76) that resides in the BTB domain of PLZF and that was important for PLZF-mediated ISG induction, thereby implicating a serine kinase in PLZF activation. Accordingly, kinase inhibitor studies implicate the serine kinase JNK as a potential activator of PLZF.

Recognition of PLZF-binding sites in proximity to ISRE suggests cooperation between canonical IFN transcription factors and PLZF. Only promoters containing both regulatory elements show both PLZF- and IFN-dependent expression. Experiments in STAT1-deficient cells demonstrate that this factor is required for PLZF-dependent transcriptional induction, as expected in IFN signaling. A direct comparison of PLZF-independent and -dependent genes demonstrated that tissue-specific expression patterns of the closely related ISGs IFIT1 and IFIT2 may be determined by PLZF. We demonstrated that PLZF associates with other essential cofactors, PML and HDAC1. Consequently, we propose a model whereby PLZF functions to stabilize a transcription complex that minimally includes STATs, HDAC1, and PML to mediate the expression of specific ISGs.

Although only a subset of ISGs is regulated by PLZF, the observed impairment is physiologically critical because it is sufficient to severely compromise the antiviral immune response. We showed this immune impairment was due to direct defects in key IFN-mediated antiviral factors and to indirect mechanisms that modulate NK cell activity. The reduced viral load in the presence of PLZF and IFN suggests that IFN-improved survival after SFV infection requires PLZF. This correlates with regulation of the expression of the antiviral mediator OAS1. OAS1 combined with the ribonuclease L (RNaseL) constitutes an antiviral RNA decay pathway previously demonstrated to regulate SFV infection (Silverman, 2007). Impaired induction of other ISGs such as IFIT2 and RSAD2, which have recently been shown to function as antiviral effectors, was also found (Borden et al., 2007). Other ISGs identified as having impaired induction in *Zbtb16*$^{-/-}$ cells, most pertinently CXCL10, do not have a direct antiviral function. CXCL10 has been demonstrated, with other chemokines, to regulate NK cell function (Biron et al., 1999). A recent study comparing wild-type and *Cxcl10*$^{-/-}$ mice has shown that CXCL10 expression promotes protection from coronavirus-induced neurological and liver disease (Walsh et al., 2007). Furthermore, a study using *Cxcl9*$^{-/-}$ and *Cxcl10*$^{-/-}$ mice has found that these chemokines are critical for the control of Herpes Simplex Virus infection through mobilization of NK cells and CTL to sites of infection (Thapa et al., 2008). IFN has an established role in the function of NK cells and influences NK activation during viral infection. Defects in NK cell activity, such as decreased production of IFN, also render mice more susceptible to viral infection (Lee et al., 2007). However, impaired NK cell function in *Zbtb16*$^{-/-}$ mice is independent of IFN production. Instead, we propose that the observed defect in NK cell activity in the *Zbtb16*$^{-/-}$ mouse is due to impairment of specific ISGs, with CXCL10 identified as a likely candidate. *Zbtb16*$^{-/-}$ mice show a marked decrease in CXCL10 expression in NK cell-rich organs, and such a decrease may lead to impaired mobility of NK cells, and therefore ineffective viral clearance. IFN-induced activation of NK cells resulted in potent cytotoxicity associated with a dramatic increase in GzmB. GzmB expression is essential for eliciting NK cell cytotoxic function and is responsible for the rapid induction of caspase-dependent apoptosis. Previous studies have demonstrated GzmB is an ISG (Cao et al., 2007; Zimmerer et al., 2007). However, the regulation of GzmB expression is not understood. Intriguingly, the GzmB promoter contains a binding site for PLZF, raising the possibility that PLZF directly regulates GzmB transcription. The findings here suggest that IFN-mediated activation of NK cells is regulated by PLZF.

Until recently, PLZF had not been ascribed any role in immune regulation. However, two recent reports demonstrate that PLZF is also expressed in NK T cells and that the transcription factor is essential to the development of these cells (Kovalovsky et al., 2008; Savage et al., 2008). Here, we showed that PLZF is also expressed in NK cells and provide evidence that PLZF is pivotal in the IFN-dependent activation of NK cells. The finding described here provides evidence that PLZF plays an important role in innate immunity via modulation of the IFN response. PLZF

regulates a key subset of ISGs with consequences for the archetypal function of IFN, to instigate resistance to virus infection.

EXPERIMENTAL PROCEDURES

Cell Lines and Treatments

RCC1 (Campbell et al., 1998) and ACHN (ATCC CRL-1611) cells were maintained in RPMI and DMEM, respectively. The U937T:PLZF45 inducible PLZF system was previously described (McConnell et al., 2003) and is based on the U937T autoregulatory tet-off system, in which withdrawal of tetracycline leads to gene expression. Actinomycin D was added to cells at a final concentration of 5 μg/ml for 8 hr prior to IFN treatment. Trichostatin A was added to cells at a final concentration of 25 ng/ml for 8–24 hr prior to IFN treatment. We obtained spleen macrophages and BMMs from age-matched WT and *Zbtb16*$^{-/-}$ mice as previously described (Barna et al., 2000). BMMs were isolated from mice and cultured as described (Sweet et al., 2001). Cells were plated at a density of 1 × 10^7 cells/plate and were cultured for an additional 24 hr without colony-stimulating factor 1. Cells were treated with 500–1000 IU/ml of IFNα1, then collected at 3, 6, and 9 hr for gene expression analysis.

Microarray

Previously obtained data of Affymetrix HG_U95Av2 expression profiles 24 and 48 hr after PLZF expression, performed in biological triplicate, were analyzed for genes with significant changes in gene expression as a result of PLZF expression with Significance Analysis of Microarrays (SAM; http://www-stat.stanford.edu/~tibs/SAM/) (McConnell et al., 2003; Tusher et al., 2001). RNA was extracted from control and IFN-treated U937T PLZF cells with Trizol reagent (Invitrogen). Labeling and hybridization to the custom ISG cDNA array were performed as described previously (Frevel et al., 2003; Sledz and Williams, 2004). Analysis was performed with GeneSpring 5.0 (Agilent). Data were first normalized with LOWESS normalization for each experiment, and then each array was normalized to the intensity of GAPDH expression so that intensities across samples could be compared. Genes with unreliable expression intensities below 300 for the induced sample (IFN-treated, PLZF-expressing, or PLZF-expressing IFN-treated) were discarded from further analyses. Data were filtered for genes induced over 2-fold in PLZF-expressing cells, and genes whose expression was 2-fold higher with PLZF and IFN treatment over IFN treatment alone were defined as PLZF responsive. PLZF-responsive genes were partitioned into seven sets with K-means cluster analysis with a standard correlation and 100 iterations.

Quantitative Real-Time PCR

Total RNA was extracted from cells with Trizol reagent (Invitrogen), and cDNA was produced with random hexamer primers and Superscript III reverse transcriptase (Invitrogen). PCR was performed on an Applied Biosystems 7700 Prism real-time PCR machine with the manufacturer's SYBR green kit and instructions (Applied Biosystems). Expression analysis of human samples by real-time PCR was done with the primers listed in the Supplemental Experimental Procedures. The $2^{-\Delta\Delta Ct}$ method was used for analysis with the untreated sample as the reference. Quantitative-PCR (Q-PCR) was performed in mouse samples. Predeveloped TaqMan probe/primers for RASD2, IFIT1, IFIT2, 2′-5′OAS, CXCL10, and CCL5 (Applied Biosystems) were used for calculation of the threshold cycle numbers that were transformed with the cycle threshold and relative value method as described by the manufacturer and were expressed relative to 18S ribosomal RNA. Results are expressed as relative gene expression for each target gene.

Bioinformatic Analysis

To elucidate functional similarities among the genes induced by PLZF, we mined gene ontologies by using the Expression Analysis Systematic Explorer (EASE) Functional Annotation Tool Suite. Promoters were retrieved with Promoser and potential binding sites were identified with MatInspector (Genomatix Suite). Overrepresented motifs were identified with MEME and JASPAR (Bailey and Elkan, 1995; Stormo, 2000) with the "-zoop" option, which indicates "zero or one occurrence per sequence," and motif width was set between 6 and 15 bp. Gene promoters that contain the ten most frequently occurring motifs were selected for further analysis. For each of these, the positional specific scoring matrix (PSSM) generated by MEME was searched against the TRANSFAC database with the MALIGN algorithm (Haverty et al., 2004). The PLZF BTB domain was analyzed with the Conserved Domain Database and TCoffee. PLZF protein sequence was run by the NetPhos 2.0 server program for predictions of serine, threonine, and tyrosine phosphorylation sites. The above bioinformatic analyses used the web programs listed in Supplemental Experimental Procedures.

Chromatin Immunoprecipitation Assay

Chromatin immunoprecipitation assays were done in accordance with the manufacturer's instructions (Upstate Biology). The presence of the target gene promoter sequences in both the input DNA and the recovered DNA immunocomplexes was detected by quantitative PCR. The antibodies used for ChIP were against PLZF (Calbiochem) and FLAG M2 (Sigma). After reversal of the crosslinking, DNA was recovered by phenol-chloroform extraction and ethanol precipitation and then used in a PCR. The sequences of the primers used for the PCR are listed in the Supplemental Experimental Procedures. PCR for IFIT2, RSAD2, and ISG15 was performed with a Sybr Green PCR mastermix (AP Biotech) on an iCycler PCR machine (Biorad).

Immunoprecipitation and Immunoblotting Analysis

For immunoprecipitation, cells were lysed with triple detergent lysis buffer and incubated with antibodies (anti-PLZF and anti-FLAG) as indicated. Antibody complexes were isolated with protein A/G-agarose beads (Pharmacia Biotech), and immunocomplexes were analyzed by SDS-PAGE and immunoblotting with anti-phospho Ser, anti-phosphoTyr (Upstate), anti-PLZF, anti-PML, anti-HDAC1, or anti-HDAC4. Expression of PLZF was assessed by immunoblotting with anti-PLZF (Calbiochem). Protein bands were detected and quantified on a Li-Cor Odyssey infrared imaging system or exposure of the membrane to BioMax autoradiographic film (Kodak).

RNAi-Mediated PLZF Knockdown

Knockdown of PLZF was induced by transfection of BLOCK-iT Pol II miR RNAi Expression Vector (RNAi PLZF plasmids targeting two different sequences in PLZF, and LacZ as control). The miRNA (plzf) target sequences were: miRNAi plzf13 (437-456), 5′-TGCTGTATAGTGTTGACTATTGCGGTTTTGGCCACTG ACTGACCGCAATAGTCAACACTATA-3′; and miRNAi plzf24 (1116-1135), 5′-TGCTGTAGTGTAGCTCCCTAGCACGTTTTGGCCACTGACTGACGTGCTA GGGAGCTACACTA-3′. Starting 24 hr after transfection, untransfected cells were eliminated by culturing the cells in the presence of 10 μg/ml blasticidin for 10–14 days. Total cellular RNA was isolated and whole-cell lysates were used for immunoblotting. The efficiency of the knockdown was assessed at the protein level by immunoblotting.

Transfection Assay and Luciferase Assays

The RASD2 luciferase reporter was provided by K. Fitzgerald (Severa et al., 2006), and the IFIT2 luciferase reporter was cloned by PCR. All plasmids used in the transfection assay were prepared with the endotoxin-free plasmid Maxi-kit (QIAGEN). A total 2 × 10^5 RCC1 or ACNH cells were incubated overnight. The wild-type and mutant RSAD2 promoter reporter gene vector (1 μg), along with 0.2 μg of a phRL-TK Synthetic Renilla expression vector, were transfected into cells with Fugene 6 (Roche). After transfection for 24 hr, the cells were harvested and lysed. Luciferase activity was generated with luciferase substrate and read out in opaque 96-well plates with a plate-reading luminometer. phRL-TK Synthetic Renilla was cotransfected for normalization of transfection efficiency. Experiments were performed in triplicate.

Immunofluorescence

Approximately 1 to 2 × 10^5 cells were seeded in Chamber slides (Lab-Tek II, Nalge Nunc International). The 60%–80% confluent culture of cells was treated with IFNα for 2–4 hr. The cells were then fixed with 4% paraformaldehyde and blocked with CAS blocking solution (Zymed). The cells were incubated with the PML (Santa Cruz) primary antibody, incubated sequentially with FITC-conjugated anti-rabbit secondary antibodies (Molecular Probes), and analyzed by fluorescence or confocal microscopy (Leica Instruments).

Antivirus Assay

Wild-type and *Zbtb16*$^{-/-}$ primary MEFs were generated. Cells were seeded into 96-well plates at 1 × 10^4 cells/well and incubated overnight, treated with serial dilutions of mouse IFN-α1 for 16 hr, and challenged with SFV virus (10^5–10^7 plaque-forming units [pfu]) for an additional 48 and 72 hr. Viral titers were determined as the dilution at which 50% death occurred and are expressed as $\log_{10}$ titers or as "fold dilution" (Fenner et al., 2006). Cells were fixed with cold methanol and stained with crystal violet, before optical density at 620 nm was read.

Viral Infection of Mice

Pups between 5 and 6 days of age were injected intraperitoneally (i.p.) with 50 μl SFV at 10×, 30×, and 100× $TCID_{50}$, determined by CPE bioassay of mouse L929 cell cultures. Some mice were preinjected with mouse IFNα 6 hr before viral infection. The mouse IFNα titer was verified in a CPE-reduction bioassay. Experiments with wild-type and *Zbtb16*$^{-/-}$ mice used littermate controls and were conducted by researchers "blinded" to experimental conditions, with genotypes being determined after completion of the experiments. Mice were monitored at 3–6 hr intervals and resistance was recorded for up to 3 weeks. Viral titers of each organ were measured at day 3 of SFV infection and IFN pretreatment (Fenner et al., 2006). For in vivo infections with EMCV, 500 pfu were injected i.p. into *Zbtb16*$^{-/-}$ mice and wild-type littermate controls. These studies were approved by the Monash University Monash Medical Centre A Animal Ethics Committee (Melbourne, Australia).

Serum Interferon Assays

Serum samples from neonatal mice were diluted in semi-$\log_{10}$ steps in duplicate into 96-well plates containing L929 cell monolayers. The medium was removed 16 hr later and SFV added at a concentration of 10× $TCID_{50}$ in fresh RPMI medium. Plates were subsequently incubated for 48–72 hr, after which they were assigned scores for CPE. This assay measures the activity of all type I and type II interferons. The interferon activity (IU/ml) was calculated by comparison of the titer of the sample with a laboratory IFNα standard calibrated to the National Institutes of Health reference standard Ga02-901-511.

Cytotoxicity Assay

This flow cytometric method, previously described by Lecoeur et al. (2001), entails labeling effector cells with carboxy-fluorescein diacetate succinimidyl ester (CFSE) so that they could be discriminated from target cells, then adding 7-amino-actinomycin D (7-AAD) so that killed targets could be labeled. Mice were injected i.p. with 0.1 ml of PBS containing poly(I:C) (10 μg/mouse) or IFNα (1 × 10^5 IU/mouse), and splenocytes were harvested after 24 or 60 hr, respectively, and labeled with CFSE. In vitro NK lysis was monitored by incubation of different numbers of CFSE-labeled effector cells with 1 × 10^4 target cells (YAC-1 cells) at 37°C for 4 hr. In parallel, target cells were incubated alone for basal apoptosis measurement. Immediately before analysis, 1 μg/ml (final concentration) of 7-AAD was added to each sample and incubated for 20 min. The percentage of apoptotic (7-AAD^{lo}+7-AAD^{hi}) cells is used for calculating the percentage of specific lysis according to the following formula: % specific lysis = 100 × (% sample lysis – % basal lysis)/(100 – % basal lysis). Sample lysis is the cell lysis in the presence of effectors at a given E:T ratio, and basal lysis is the cell lysis in the absence of effectors.

Cell Isolation and Stimulation

Spleens were harvested and single-cell suspensions were generated. Red blood cells were lysed and the cells were washed in RPMI medium. For in vitro cytokine stimulation, splenocytes were plated at 10 × 10^6/ml in 24-well plates in 1000 U/ml IL-2. Cells were harvested by pipetting with cold PBS after 48 hr and analyzed by flow cytometry. For cell sorting, splenocytes were surface stained with anti-NK1.1, anti-CD3, and anti-B220 (BD Biosciences PharMingen), and CD3$^+$NK1.1$^-$, CD3$^-$NK1.1$^+$, or B220 cells were isolated by cell sorter (routinely ≥99% pure).

Intracellular Staining and Flow Cytometry

Splenocytes or tissue mononuclear cells were stained for surface markers (NK1.1) and intracellular Gzmb as described (eBioscience Foxp3 staining protocol) with directly conjugated Gzmb (1:400 dilution) monoclonal antibodies. Sample data were acquired on a Cytek-modified FACScan (BD) flow cytometer, and isotype controls were used to set quadrant gates.

ACCESSION NUMBERS

Microarray data are available from the National Center for Biotechnology Information Gene Expression Omnibus (GEO) under accession number GSE 16197.

SUPPLEMENTAL DATA

Supplemental Data include Supplemental Experimental Procedures, 5 tables, and 14 figures and can be found with this article online at http://www.cell.com/immunity/supplemental/S1074-7613(09)00236-2.

ACKNOWLEDGMENTS

We thank K. Fitzgerald for the RASD2-luc constructs, P. Hertzog and P. Fitzgerald-Bocarsly for helpful advice, and N. de Weerd, S. Samarajiwa, and J. Gould for mouse IFNα and SFV virus. We thank I. Harper, S. Firth, and C. Lo (Monash Micro Imaging) for the confocal microscopic analysis and M. Gantier, D. Wang, D. Wu, and J. Ou for technical assistance. We also thank F. Cribbin for critical reading and preparation of the manuscript. This work was supported by grants from the National Health and Medical Research Council of Australia (436814 to B.R.G.W.) and the National Institutes of Health (P01 CA062220 and R01 AI034039 to B.R.G.W.).

Received: December 2, 2008
Revised: March 23, 2009
Accepted: April 17, 2009
Published online: June 11, 2009

REFERENCES

Ahmad, K.F., Engel, C.K., and Prive, G.G. (1998). Crystal structure of the BTB domain from PLZF. Proc. Natl. Acad. Sci. USA *95*, 12123–12128.

Bailey, T.L., and Elkan, C. (1995). The value of prior knowledge in discovering motifs with MEME. Proc. Int. Conf. Intell. Syst. Mol. Biol. *3*, 21–29.

Ball, H.J., Melnick, A., Shaknovich, R., Kohanski, R.A., and Licht, J.D. (1999). The promyelocytic leukemia zinc finger (PLZF) protein binds DNA in a high molecular weight complex associated with cdc2 kinase. Nucleic Acids Res. *27*, 4106–4113.

Barna, M., Hawe, N., Niswander, L., and Pandolfi, P.P. (2000). Plzf regulates limb and axial skeletal patterning. Nat. Genet. *25*, 166–172.

Biron, C.A., Nguyen, K.B., Pien, G.C., Cousens, L.P., and Salazar-Mather, T.P. (1999). Natural killer cells in antiviral defense: Function and regulation by innate cytokines. Annu. Rev. Immunol. *17*, 189–220.

Borden, E.C., Sen, G.C., Uze, G., Silverman, R.H., Ransohoff, R.M., Foster, G.R., and Stark, G.R. (2007). Interferons at age 50: Past, current and future impact on biomedicine. Nat. Rev. Drug Discov. *6*, 975–990.

Campbell, C.E., Kuriyan, N.P., Rackley, R.R., Caulfield, M.J., Tubbs, R., Finke, J., and Williams, B.R. (1998). Constitutive expression of the Wilms tumor suppressor gene (WT1) in renal cell carcinoma. Int. J. Cancer *78*, 182–188.

Cao, X., Cai, S.F., Fehniger, T.A., Song, J., Collins, L.I., Piwnica-Worms, D.R., and Ley, T.J. (2007). Granzyme B and perforin are important for regulatory T cell-mediated suppression of tumor clearance. Immunity *27*, 635–646.

Chang, H.M., Paulson, M., Holko, M., Rice, C.M., Williams, B.R., Marie, I., and Levy, D.E. (2004). Induction of interferon-stimulated gene expression and antiviral responses require protein deacetylase activity. Proc. Natl. Acad. Sci. USA *101*, 9578–9583.

Chauchereau, A., Mathieu, M., de Saintignon, J., Ferreira, R., Pritchard, L.L., Mishal, Z., Dejean, A., and Harel-Bellan, A. (2004). HDAC4 mediates transcriptional repression by the acute promyelocytic leukaemia-associated protein PLZF. Oncogene *23*, 8777–8784.

David, G., Alland, L., Hong, S.H., Wong, C.W., DePinho, R.A., and Dejean, A. (1998). Histone deacetylase associated with mSin3A mediates repression by the acute promyelocytic leukemia-associated PLZF protein. Oncogene *16*, 2549–2556.

Day, P.M., Baker, C.C., Lowy, D.R., and Schiller, J.T. (2004). Establishment of papillomavirus infection is enhanced by promyelocytic leukemia protein (PML) expression. Proc. Natl. Acad. Sci. USA *101*, 14252–14257.

Dong, S., Zhu, J., Reid, A., Strutt, P., Guidez, F., Zhong, H.J., Wang, Z.Y., Licht, J.D., Waxman, S., Chomienne, C., et al. (1996). Amino-terminal protein-protein interaction motif (POZ-domain) is responsible for activities of the promyelocytic leukemia zinc finger-retinoic acid receptor-alpha fusion protein. Proc. Natl. Acad. Sci. USA *93*, 3624–3629.

Fehniger, T.A., Cai, S.F., Cao, X., Bredemeyer, A.J., Presti, R.M., French, A.R., and Ley, T.J. (2007). Acquisition of murine NK cell cytotoxicity requires the translation of a pre-existing pool of granzyme B and perforin mRNAs. Immunity *26*, 798–811.

Fenner, J.E., Starr, R., Cornish, A.L., Zhang, J.G., Metcalf, D., Schreiber, R.D., Sheehan, K., Hilton, D.J., Alexander, W.S., and Hertzog, P.J. (2006). Suppressor of cytokine signaling 1 regulates the immune response to infection by a unique inhibition of type I interferon activity. Nat. Immunol. *7*, 33–39.

Frevel, M.A., Bakheet, T., Silva, A.M., Hissong, J.G., Khabar, K.S., and Williams, B.R. (2003). p38 Mitogen-activated protein kinase-dependent and -independent signaling of mRNA stability of AU-rich element-containing transcripts. Mol. Cell. Biol. *23*, 425–436.

Goh, K.C., Haque, S.J., and Williams, B.R. (1999). p38 MAP kinase is required for STAT1 serine phosphorylation and transcriptional activation induced by interferons. EMBO J. *18*, 5601–5608.

Goodbourn, S., Didcock, L., and Randall, R.E. (2000). Interferons: Cell signalling, immune modulation, antiviral response and virus countermeasures. J. Gen. Virol. *81*, 2341–2364.

Guidez, F., Howell, L., Isalan, M., Cebrat, M., Alani, R.M., Ivins, S., Hormaeche, I., McConnell, M.J., Pierce, S., Cole, P.A., et al. (2005). Histone acetyltransferase activity of p300 is required for transcriptional repression by the promyelocytic leukemia zinc finger protein. Mol. Cell. Biol. *25*, 5552–5566.

Handwerger, K.E., and Gall, J.G. (2006). Subnuclear organelles: New insights into form and function. Trends Cell Biol. *16*, 19–26.

Haque, S.J., and Williams, B.R. (1998). Signal transduction in the interferon system. Semin. Oncol. *25*, 14–22.

Haverty, P.M., Frith, M.C., and Weng, Z. (2004). CARRIE web service: Automated transcriptional regulatory network inference and interactive analysis. Nucleic Acids Res. *32*, w213–w216.

Holko, M., and Williams, B.R. (2006). Functional annotation of IFN-alpha-stimulated gene expression profiles from sensitive and resistant renal cell carcinoma cell lines. J. Interferon Cytokine Res. *26*, 534–547.

Hong, S.H., David, G., Wong, C.W., Dejean, A., and Privalsky, M.L. (1997). SMRT corepressor interacts with PLZF and with the PML-retinoic acid receptor alpha (RARalpha) and PLZF-RARalpha oncoproteins associated with acute promyelocytic leukemia. Proc. Natl. Acad. Sci. USA *94*, 9028–9033.

Isaacs, A., Lindenmann, J., and Valentine, R.C. (1957). Virus interference. II. Some properties of interferon. Proc. R. Soc. Lond. B. Biol. Sci. *147*, 268–273.

Koken, M.H., Reid, A., Quignon, F., Chelbi-Alix, M.K., Davies, J.M., Kabarowski, J.H., Zhu, J., Dong, S., Chen, S.J., Chen, Z., et al. (1997). Leukemia-associated retinoic acid receptor alpha fusion partners, PML and PLZF, heterodimerize and colocalize to nuclear bodies. Proc. Natl. Acad. Sci. USA *94*, 10255–10260.

Kovalovsky, D., Uche, O.U., Eladad, S., Hobbs, R.M., Yi, W., Alonzo, E., Chua, K., Eidson, M., Kim, H.J., Im, J.S., et al. (2008). The BTB-zinc finger transcriptional regulator PLZF controls the development of invariant natural killer T cell effector functions. Nat. Immunol. *9*, 1055–1064.

Labbaye, C., Quaranta, M.T., Pagliuca, A., Militi, S., Licht, J.D., Testa, U., and Peschle, C. (2002). PLZF induces megakaryocytic development, activates Tpo receptor expression and interacts with GATA1 protein. Oncogene *21*, 6669–6679.

Lecoeur, H., Fevrier, M., Garcia, S., Riviere, Y., and Gougeon, M.L. (2001). A novel flow cytometric assay for quantitation and multiparametric characterization of cell-mediated cytotoxicity. J. Immunol. Methods *253*, 177–187.

Lee, S.H., Miyagi, T., and Biron, C.A. (2007). Keeping NK cells in highly regulated antiviral warfare. Trends Immunol. *28*, 252–259.

McConnell, M.J., Chevallier, N., Berkofsky-Fessler, W., Giltnane, J.M., Malani, R.B., Staudt, L.M., and Licht, J.D. (2003). Growth suppression by acute promyelocytic leukemia-associated protein PLZF is mediated by repression of c-myc expression. Mol. Cell. Biol. *23*, 9375–9388.

McLoughlin, P., Ehler, E., Carlile, G., Licht, J.D., and Schäfer, B.W. (2002). The LIM-only protein DRAL/FHL2 interacts with and is a corepressor for the promyelocytic leukemia zinc finger protein. J. Biol. Chem. *277*, 37045–37053.

Melnick, A., Ahmad, K.F., Arai, S., Polinger, A., Ball, H.J., Borden, K.L., Carlile, G.W., Prive, G.G., and Licht, J.D. (2000a). In-depth mutational analysis of the promyelocytic leukemia zinc finger BTB/POZ domain reveals motifs and residues required for biological and transcriptional functions. Mol. Cell. Biol. *20*, 6550–6567.

Melnick, A.M., Westendorf, J.J., Polinger, A., Carlile, G.W., Arai, S., Ball, H.J., Lutterbach, B., Hiebert, S.W., and Licht, J.D. (2000b). The ETO protein disrupted in t(8;21)-associated acute myeloid leukemia is a corepressor for the promyelocytic leukemia zinc finger protein. Mol. Cell. Biol. *20*, 2075–2086.

Pestka, S., Langer, J.A., Zoon, K.C., and Samuel, C.E. (1987). Interferons and their actions. Annu. Rev. Biochem. *56*, 727–777.

Qiu, Y., Zhao, Y., Becker, M., John, S., Parekh, B.S., Huang, S., Hendarwanto, A., Martinez, E.D., Chen, Y., Lu, H., et al. (2006). HDAC1 acetylation is linked to progressive modulation of steroid receptor-induced gene transcription. Mol. Cell *22*, 669–679.

Regad, T., and Chelbi-Alix, M.K. (2001). Role and fate of PML nuclear bodies in response to interferon and viral infections. Oncogene *20*, 7274–7286.

Sadler, A.J., and Williams, B.R. (2008). Interferon-inducible antiviral effectors. Nat. Rev. Immunol. *8*, 559–568.

Savage, A.K., Constantinides, M.G., Han, J., Picard, D., Martin, E., Li, B., Lantz, O., and Bendelac, A. (2008). The transcription factor PLZF directs the effector program of the NKT cell lineage. Immunity *29*, 391–403.

Senbonmatsu, T., Saito, T., Landon, E.J., Watanabe, O., Price, E.J., Roberts, R.L., Imboden, H., Fitzgerald, T.G., Gaffney, F.A., and Inagami, T. (2003). A novel angiotensin II type 2 receptor signaling pathway: Possible role in cardiac hypertrophy. EMBO J. *22*, 6471–6482.

Severa, M., Coccia, E.M., and Fitzgerald, K.A. (2006). Toll-like receptor-dependent and -independent viperin gene expression and counter-regulation by PRDI-binding factor-1/BLIMP1. J. Biol. Chem. *281*, 26188–26195.

Shey, M.R., and Ballas, Z.K. (2008). Assessment of natural killer (NK) and NKT cells in murine spleens and livers. Methods Mol. Biol. *447*, 259–276.

Silverman, R.H. (2007). Viral encounters with 2′,5′-oligoadenylate synthetase and RNase L during the interferon antiviral response. J. Virol. *81*, 12720–12729.

Sledz, C.A., and Williams, B.R. (2004). RNA interference and double-stranded-RNA-activated pathways. Biochem. Soc. Trans. *32*, 952–956.

Stadler, M., Chelbi-Alix, M.K., Koken, M.H., Venturini, L., Lee, C., Saib, A., Quignon, F., Pelicano, L., Guillemin, M.C., Schindler, C., et al. (1995). Transcriptional induction of the PML growth suppressor gene by interferons is mediated through an ISRE and a GAS element. Oncogene *11*, 2565–2573.

Stark, G.R., Kerr, I.M., Williams, B.R., Silverman, R.H., and Schreiber, R.D. (1998). How cells respond to interferons. Annu. Rev. Biochem. *67*, 227–264.

Stormo, G.D. (2000). DNA binding sites: Representation and discovery. Bioinformatics *16*, 16–23.

Sweet, M.J., Leung, B.P., Kang, D., Sogaard, M., Schulz, K., Trajkovic, V., Campbell, C.C., Xu, D., and Liew, F.Y. (2001). A novel pathway regulating lipopolysaccharide-induced shock by ST2/T1 via inhibition of Toll-like receptor 4 expression. J. Immunol. *166*, 6633–6639.

Tenoever, B.R., Ng, S.L., Chua, M.A., McWhirter, S.M., Garcia-Sastre, A., and Maniatis, T. (2007). Multiple functions of the IKK-related kinase IKKepsilon in interferon-mediated antiviral immunity. Science *315*, 1274–1278.

Terenzi, F., White, C., Pal, S., Williams, B.R., and Sen, G.C. (2007). Tissue-specific and inducer-specific differential induction of ISG56 and ISG54 in mice. J. Virol. *81*, 8656–8665.

Thapa, M., Welner, R.S., Pelayo, R., and Carr, D.J. (2008). CXCL9 and CXCL10 expression are critical for control of genital herpes simplex virus type 2 infection through mobilization of HSV-specific CTL and NK cells to the nervous system. J. Immunol. *180*, 1098–1106.

Tusher, V.G., Tibshirani, R., and Chu, G. (2001). Significance analysis of microarrays applied to the ionizing radiation response. Proc. Natl. Acad. Sci. USA *98*, 5116–5121.

van Boxel-Dezaire, A.H., Rani, M.R., and Stark, G.R. (2006). Complex modulation of cell type-specific signaling in response to type I interferons. Immunity *25*, 361–372.

Walsh, K.B., Edwards, R.A., Romero, K.M., Kotlajich, M.V., Stohlman, S.A., and Lane, T.E. (2007). Expression of CXC chemokine ligand 10 from the mouse hepatitis virus genome results in protection from viral-induced neurological and liver disease. J. Immunol. *179*, 1155–1165.

Zimmerer, J.M., Lesinski, G.B., Radmacher, M.D., Ruppert, A., and Carson, W.E., 3rd. (2007). STAT1-dependent and STAT1-independent gene expression in murine immune cells following stimulation with interferon-alpha. Cancer Immunol. Immunother. *56*, 1845–1852.

Zupkovitz, G., Tischler, J., Posch, M., Sadzak, I., Ramsauer, K., Egger, G., Grausenburger, R., Schweifer, N., Chiocca, S., Decker, T., and Seiser, C. (2006). Negative and positive regulation of gene expression by mouse histone deacetylase 1. Mol. Cell. Biol. *26*, 7913–7928.